Al-Rafidain Engineering Journal (AREJ) Vol.27, No.1, March 2022, pp.116-126

Effects of Key Processing Parameters of Continuous Drive Rotary Friction Welding on Thermal Characteristics of Similar and Dissimilar Joints

Faris Ibrahim Salih faris.enp67@student.uomosul.edu.iq
Amir Sultan Dawood asdawood54@gmail.com
Abdulhaqq A. Hamid abdulhaqqhamid@uomosul.edu.iq

Mechanical Engineering Department, Collage of Engineering, University of Mosul

Received: 19/10/2021 Accepted: 18/12/2021

ABSTRACT

In this research study, numerical modeling was present to describe the effect of key processing parameters of continuous drive rotary friction welding (CDRFW) on thermal characteristics of similar aluminum alloy joint and dissimilar aluminum alloy /low carbon mild steel joint, using (ANSYS). A mathematical model was made to describe the heat generated in the workpiece due to the frictional force and the plastic deformation, and the heat transfer throw workpiece was described based on the Fourier law of heat conduction. The parameters were: Frictional pressure (P_1), forging pressure (P_2), frictional time (t_1), forging time (t_2), and rotational speed (N). A range of welding parameters was taken. The results show that with increases in welding parameters, the welding temperature at the interface region and the axial shortening will increase for both similar and dissimilar joints. For similar and dissimilar joints, frictional pressure and rotational speed have the most effect on maximum temperature at the interface, frictional time affects less while forging pressure and forging time have no effect on maximum temperature at the interface. For similar and dissimilar joints the most influential parameter on axial shortening was frictional pressure, with little effect for forging time.

Keywords:

Numerical modeling; Rotary friction welding; Temperature profile; Axial shortening; Welding parameters.

https://rengj.mosuljournals.com

1. INTRODUCTION

Friction welding is the process of joining materials without reaching melting point for this reason it's called a solid-state process and it's the most effective process for similar and dissimilar joining with very high joint strength. Friction welding is a pressure variation method, in which with the help of friction that causes heat generated, the welded joint is formed by joint plastic deformation of the pieces to be welded without melting the metal. Thermo-mechanical work involves friction welding which results in grain refinement of the weld region. Friction welding is characterized by low heat requite, easy application, and material saving. Friction welding is used to join different shapes like the rod to rod, rod to plate, etc. [1].

Rotary friction welding (RFW) is the oldest and most commonly used method and can be defined as a solid-state process for joining materials in which the rotational movement at the interface between the two materials generates heat, the heat softens the material and the material flows to the edges, and this material flow is necessary to remove contaminants and other oxides, etc. from the weld interface [1]. In rotary friction welding, one part of the workpiece is held stationary while the other rotates at a high necessary speed.

The main key variables of direct drive friction welding are: axial pressure, rotational speed and welding time. These variables determine how much energy is introduced in the welding region and the rate of heat generation at the interface. It should be noted that during the different stages of welding, the heat generation rate at interface is not constant but the difference is not great, so many authors assume it constant. During the welding process, resistance torque and axial shortening will also change [2]. The changes in the characteristics of friction welding parameters over time are shown in Fig. 1.

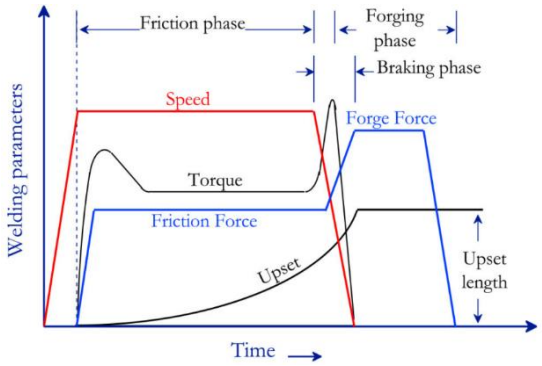

Figure 1: Show the variation of the characteristics of friction welding parameters over time. [2]

2. HEAT AFFECTED ZONE (HAZ)

The heat affected zone (HAZ) it is the zone that is affected by heat, whether this effect is apparent or not, and it is divided into four zones, as shown in Fig. 2, the zones are: (i) contact zone – is a thin area where friction occurs, with a great strain and strain rate, the material flow is mainly deform, with large amplitude. (ii) Fully plasticized zone – there is a plastic deformation, but it is smaller than the contact zone, It also has a large strain and strain rate. (iii) Partial deformation zone – limited plastic deformation compared to regions (i) and (ii), strain and strain rate are significantly reduced. (iv) un deformed zone – no material flow (no plastic deformation), but the microstructure will be affected by temperature [3].

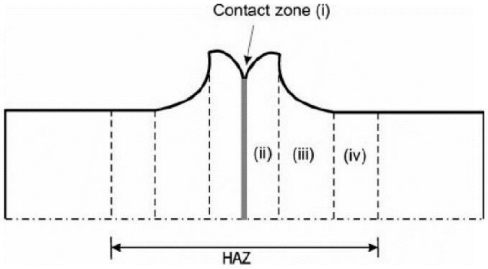

Figure 2: Shows HAZ for RFW process. [3]

3. MATHEMATICAL MODELLING

The mathematical model was made to find the heat generated at the interface and the heat transfer through the workpieces during the rotary friction welding process.

3.1 General assumptions:

The heat generation on the interface region and pressure applied is assumed to be uniform. Since the total welding time in this process is usually very short and the contact surface is not exposed to the surrounding environment, the heat loss through convection and radiation is neglected. The heat input is considered constant throughout the process. The material is assumed to be homogeneous and isotropic. Dynamic friction coefficient considered constant throughout the process.

3.2 Heat generation

The temperature of the interface weld zone rises sharply in the rotary friction welding process, due to intemperate friction and plastic deformation of the work pieces in a very short time. In order to calculate the temperature distribution, the heat transfer analysis is performed by considering that, heat generation consists of two parts, heat generation due to the friction at the interface and the heat generated due to plastic deformation.

3.2.1 Heat generation by friction

The frictional heat generated rate per unit volume ($\dot{q}_f$) is given as: [4] [5] [6]

$$\dot{q}_f = \frac{2}{3L}\mu p R \omega \qquad (1)$$

Where (μ) is dynamic friction coefficient, (p) is the axial pressure, (R) is the total radius of the workpiece and (ω) is angular velocity.

3.2.2 Heat generation by plastic deformation

At first, all heat generation from the rotary friction welding process came from the friction at the interface, and with raising the temperature the yield stress reduce until it became less than flow stress, and then the plastic deformation start. In the analysis of material deformation, the relationship between the thermal strain and the material will be affected by the temperature distribution during the heat transfer process, and the deformation of the material will change boundary conditions, the heat transfer space, and energy transfer [4]. Due to the low value of plastic heat generation compares with friction heat generation and the difficulty of calculation, many researchers were neglected it. In this current research, the laws governing the heat resulting from the deformation were clarified, and they were calculated implicitly through the ANSYS program. The rate of heat generation per unit volume due to plastic deformation ($\dot{q}_p$) can be defined as: [4] [5] [6]

$$\dot{q}_p = \beta \sigma_e \dot{\varepsilon} \qquad (2)$$

Where (β) is the thermal efficiency, and according to the theory of the plastic deformation,

most of the work came from plastic deformation is converted into heat, and usually the thermal efficiency (β) is set to (0.9), the rest of the energy is stored in the form of vacancies and dislocations [7]. For this research the thermal efficiency (β) was taken (0.9) as well. (σ_e) is the equivalent flow stress and defined as the instantaneous value of stress required to continue plastically deforming a material, and it must exceed the yield stress (σ_S) to start the plastic deformation in the work piece.

The equivalent flow stress can be found from Johnson-Cook damage model as [8].

$$\sigma_e = (A + B\varepsilon^n) * \left[1 + C\ln\left(1 + \frac{\dot{\varepsilon}}{\dot{\varepsilon}_0}\right)\right] * \left[1 - \left(\frac{T - T_{\text{room}}}{T_{\text{melt}} - T_{\text{room}}}\right)^m\right] \quad (3)$$

Where (ε), ($\dot{\varepsilon}$) and ($\dot{\varepsilon}_0$) are strain, strain rate and reference strain rate respectively. (T_{melt}) and (T_{room}) are melting temperature and room temperature respectively. A, B, C, n and m are material dependent constants and they obtained from experiment, where A is the reference yield stress, B is the constant strain hardening, C is the coefficient of strengthening, n is the coefficient of strain hardening and m is the coefficient of thermal softening [8].

The total rate of heat generation per unit volume, for the welding process ($\dot{q}$) is expressed as:

$$\dot{q} = \dot{q}_f + \dot{q}_p \quad (4)$$

3.3 The heat transfer of the welding process

Based on the assumption of no heat loss through convection and radiation for the rotary friction welding process, the unsteady state Fourier law of heat conduction in the coupled heat-mechanical problems in (x) axis with no heat loss through convection and radiation can be expressed as Eq. (5): [5] [9] [10]. The sketch for the process is shown in Fig. 3.

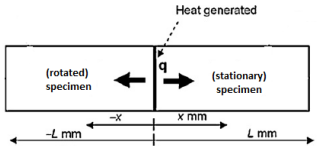

Figure 3: The boundary condition for heat conduction model. [10]

$$\alpha\frac{\partial^2 T}{\partial x^2} + u\frac{\partial T}{\partial x} + \frac{\dot{q}}{\rho c_p} = \frac{\partial T}{\partial t} \quad (5)$$

Where (T) is the temperature, (t) is the time, (ρ) is the material density, (c_p) is the specific heat capacity, (u) is the velocity of the axial shortening and (α) is thermal diffusivity and it represent the ratio of the heat conducted throw the material to heat stored per unit volume, and it formula is:

$$\alpha = \frac{k}{\rho c_p} \quad (6)$$

Where (k) is the thermal conductivity.

4. MATERIALS AND PROPERTIES

The materials used in this current research was aluminum alloy (6061-T651) and low carbon mild steel. The chemical compositions of the materials were given in the Tables (1) and (2).

Table 1: Chemical composition of aluminum alloy (6061-T651). [11]

Si	Fe	Cu	Mn	Mg	Cr	Zn	Ti	Al
0.66	0.4	0.24	0.07	0.9	0.18	0.02	0.02	base

Table 2: Chemical composition of low carbon mild steel. [12]

C	Si	Mn	P	S	Cr	Ni	MO	Cu	Al	Fe
0.19	0.37	1.57	0.023	0.027	0.06	0.03	0.01	0.04	0.046	base

During rotary friction welding, the temperature of the workpieces rises and with the change of temperature of both materials workpiece, their properties will also change. The variable properties with the temperature that took place in this research were density, thermal conductivity, specific heat, volumetric thermal expansion, young's modulus, strain rate, equivalent flow stress, and yield stress. For Al-alloy (6061-T651) the properties were taken from research work [11], for low carbon mild steel the properties were taken from research work [12]. The dynamic friction coefficient for a similar Al-alloy joint was taken as (1.4) and for dissimilar Al-alloy/mild steel joint was taken as (0.47) [13].

5. NUMERICAL SOLUTION

In this research work, the numerical simulation of the rotary friction welding was formed using (ANSYS Coupled Field Transient-2021), Coupled Field Transient is a coupled between static structure and transient thermal. The Coupled field transient is solved based on the Finite element method.

5.1 Geometry and meshing

A three-dimensional model consisting of two rods specimen's parts was created by ANSYS

with rod diameter (10 mm) and (32 mm) in length. To reduce the time of ANSYS solving, the mesh near to the interface was fine and along with the work, pieces were coarse. The number of nodes was (44825) and the number of the elements was (125308) which was a very good quality mesh with good solving time in comparison with a lower and higher number of elements that were chosen first, the model is shown in Fig. 4.

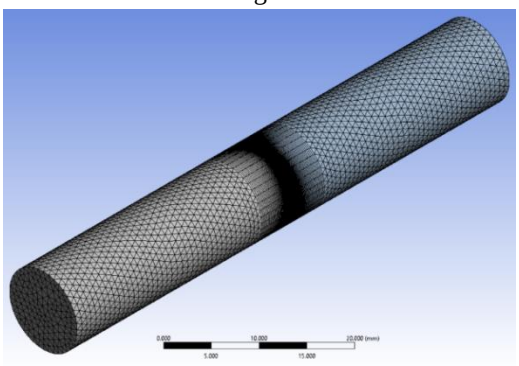

Figure 4: Show the current two rods of specimens the geometry and the mesh.

5.2 Boundary conditions

For the similar materials Al-alloy joint, one component is held stationary and the other rotates at a constant speed. The axial pressure was applied normally on the surface of the rotating part. The axial pressure was given in two steps like the actual process. For dissimilar materials Al-alloy/mild steel joint, mild steel was held stationary and Al-alloy was the component that rotated and given axial load.

5.3 RFW parameters range

The welding key parameters for rotary friction welding are, frictional pressure (P_1), frictional time (t_1), forging pressure (P_2), forging time (t_2) and rotational speed (N). Range of welding parameters for similar Al-alloy joint are: (P_1: 24-32 MPa), (P_2: 34-70 MPa), (t_1:3-7 sec), (t_2: 1 sec) and (N: 1000-1600 rpm)). Range of welding parameters for dissimilar Al-alloy / mild steel joint are: (P_1: 50-75 MPa), (P_2: 60-100 MPa), (t_1: 3-7 sec), (t_2: 1 sec) and (N: 1200-1650 rpm)).

6. RESULTS AND DISCUSSIONS

The numerical results that will be shown are, a typical result of temperature profile and axial shortening, validation of current modeling, and the effect of each processing parameter on the temperature at the interface region and the axial shortening, all for both similar and dissimilar joints. The contribution for welding parameters was presented.

6.1 Typical results of temperature profile and axial shortening

A typical result of temperature profile and axial shortening got from similar joint and for a dissimilar joint. The processing parameters are kept constant as (P_1=30 MPa, P_2=40 MPa, t_1=3 sec, t_2=1 sec and N=1500 rpm) for similar joint and for dissimilar joint, the processing parameters are kept constant as (P_1=70 MPa, P_2=80 MPa, t_1=3 sec, t_2=1 sec and N=1500 rpm). Fig. (5-a) shows the variation of temperature profile with time at the interface between the two rods weldment produced by rotary friction welding while Fig. (5-b) shows the variation of the axial shortening with time for the welded rod, both for the similar joint. It's observed that at the beginning of the welding process, the temperature rises significantly, while the decrease in length is small because of the high flow stress for both rods compare with applied axial pressure. The temperature continues to rise until it reaches a point of relative stability and this stage is called the first stage. With the temperature increasing, the flow stress for both rods will reduce, with decreasing the flow stress, the material of the rods cannot withstand the applied axial pressure, and the plastic flows outward reducing the length and this stage is called the second stage, where most of the heat is taken for plastic deformation and the temperature rise is little in this stage. The third stage begins when the rotation stops, at that moment the temperature at the interface will start decreasing and the axial pressure is increased as needed and the decreases in height become greater. With the decrease of the temperature at the interface, the flow stress increases again and overcomes the applied pressure.

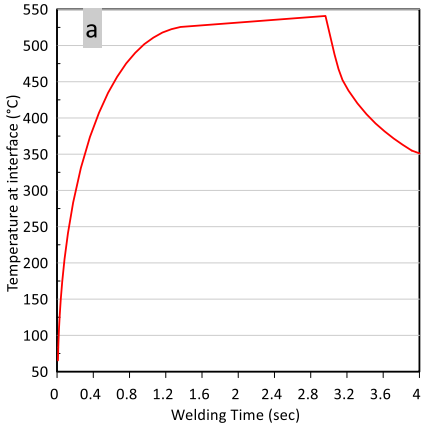

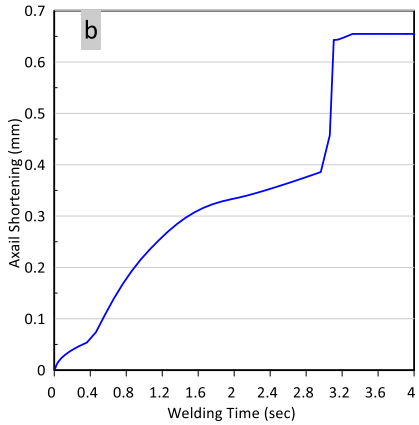

Figure 5: Temperature profile (a) and axial shortening (b), for similar joint.

For the dissimilar joint, the temperature profile with time at the interface region was shown in Fig. (6-a) while the axial shortening with time was shown in Fig. (6-b). It's noted that the welding stages for dissimilar joint have close behavior to stages of similar joint welding, but need more axial force. For dissimilar case, most of the decrease in height occurred in the second stage it could be because the forging pressure given in the third stage was close to frictional pressure.

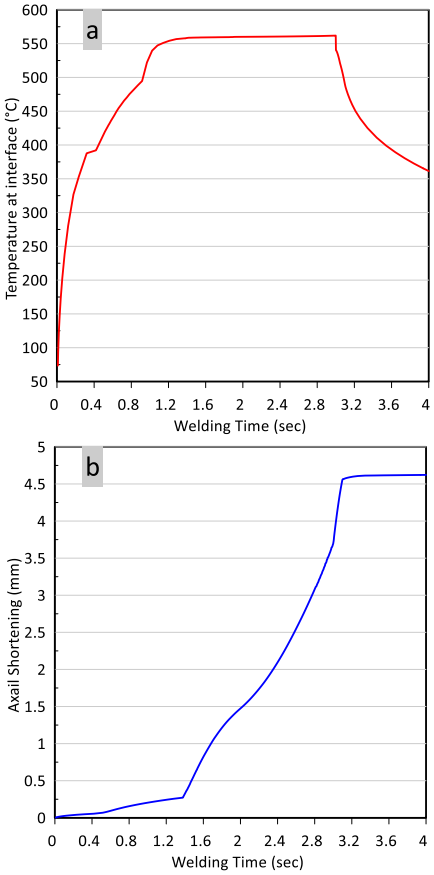

Figure 6: Temperature profile (a) and axial shortening (b), for dissimilar joint.

The typical results of temperature distribution and axial shortening were shown in from of ANSYS contour at different instants of time for similar joint in Fig. 7 and for dissimilar joint in Fig. 8.

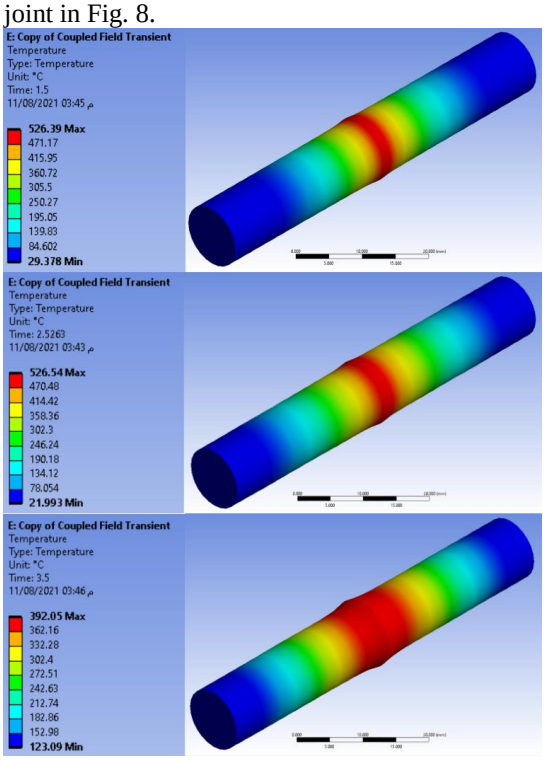

Figure 7: Temperature distribution and axial shortening at (1.5, 2.5 and 3.5 sec) for similar joint.

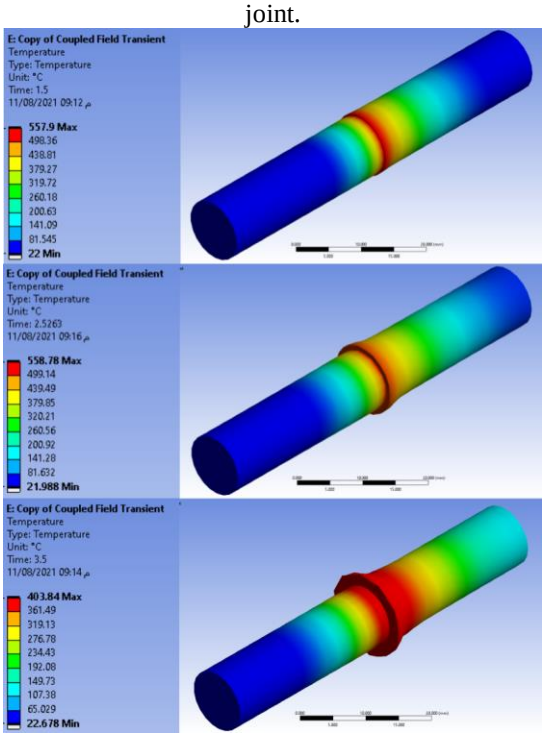

Figure 8: temperature distribution and axial shortening at (1.5, 2.5 and 3.5 sec) for dissimilar joint.

6.2 Validation of current modelling

Any result of numerical study need validation to find out the correctness of their results. The validation of current modelling was made between two numerical cases with two different experimental studies.

Case (1): the comparison was made between the numerical solutions with previous researches conducted by Xiong [14] for similar Al-alloy joint as shown in Fig.9. The rod diameter was (10 mm) and the rod length was (50 mm) for each. The processing parameters are kept constant as (P_1=29.2 MPa, P_2=34 MPa, t_1=3 sec, t_2=1 sec and N=1600 rpm). It is noticed that the temperature rise at the interface for the first stage is faster for the numerical solution compare with the experimental result. There is temperature stability in the second stage of the numerical solution with fluctuating stability of the experimental results. In the third stage, the temperature drop is more or less the same. The maximum temperature difference between the numerical and experimental results for stage two was (35.92 °C) at the time (1.82 sec). The temperature profile for the numerical solution was very smooth probably because of the assumptions that were taken with ideal conditions that do not exist in reality.

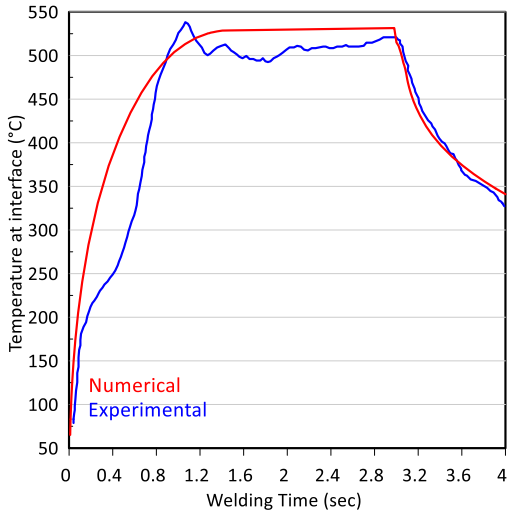

Figure 9: The temperature profile for numerical solution and previous experimental [14], for similar joint.

Case (2): the comparison was made between the numerical solutions with previous researches conducted by Seli [4] for dissimilar Al-alloy/mild steel joint as shown in Fig.10. The rod diameter was (20 mm) and the rod length was (100 mm) for each. The processing parameters are kept constant as (P_1=45 MPa, P_2=55 MPa, t_1=3.1 sec, t_2=0.9 sec and N=900 rpm). It is noticed that the temperature profile at the first stage of the experimental results is similar to the previous experimental study [4], where the temperature rise is slower than the numerical solution but the second stage is more stable compared to the previous results. The maximum temperature difference between the numerical and experimental results for stage two was (17.88 °C) at time (2.2 sec).

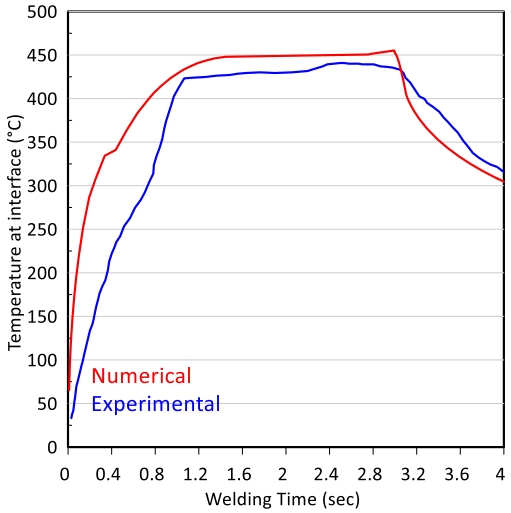

Figure 10: The temperature profile for numerical solution and previous experimental [4], for dissimilar joint.

6.3 Effect of RFW process parameters

6.3.1 Effect of frictional pressure (P_1)

The temperature profile with time at the interface area between the two rods at different frictional time were shown in Fig. (11-a) for similar Al-alloy joints and in Fig. (12-a) for dissimilar Al-alloy/mild steel joints. The axial shortening with time for the welded rod at different frictional time were shown in Fig. (11-b) for similar Al-alloy joints and in Fig. (12-b) for dissimilar Al-alloy/mild steel joints. The processing parameters for similar joint are kept constant as (P_2=40 MPa, t_1=3 sec, t_2=1 sec and N=1500 rpm) and for dissimilar joint are kept constant as (P_2=80 MPa, t_1=3 sec, t_2=1 sec and N=1500 rpm). It is observed that as the frictional pressure increases, the temperature at the interface will increase, and the axial shortening will also increase for both similar and dissimilar joints. In dissimilar joints, the increase in temperature between each case was higher than in similar joints. In a similar joint most of the decrease in length occurred in the third stage while in a dissimilar joint most of the decrease in length occurred in the second stage, it could be because the forging pressure given in the third stage was close to frictional pressure in a dissimilar joint case.

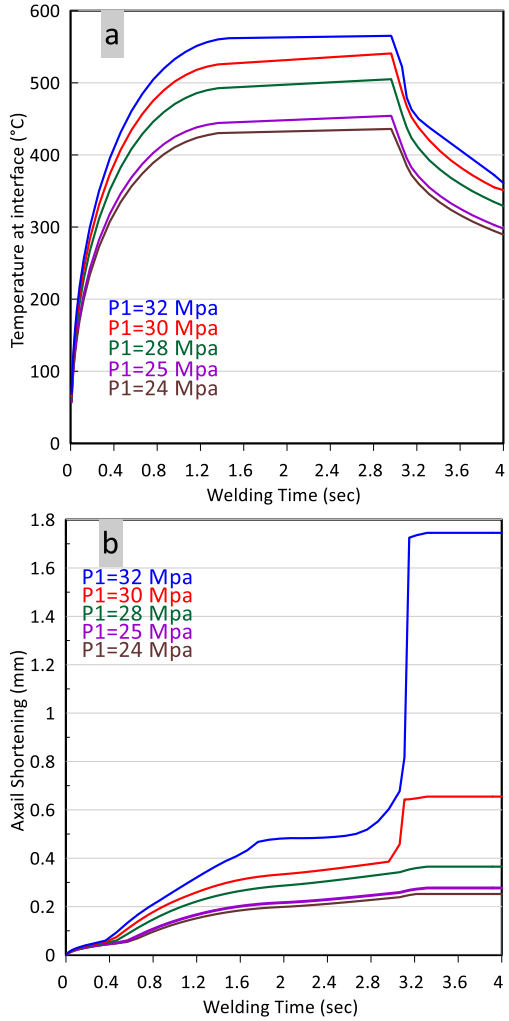

Figure 11: (a) Temperature profile variation and (b) axial shortening variation, at different frictional pressures for similar joint.

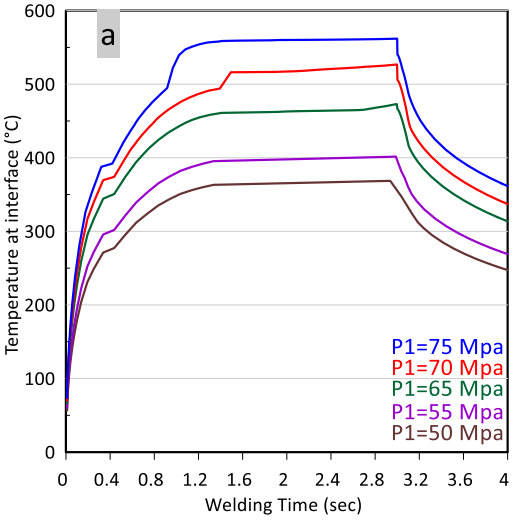

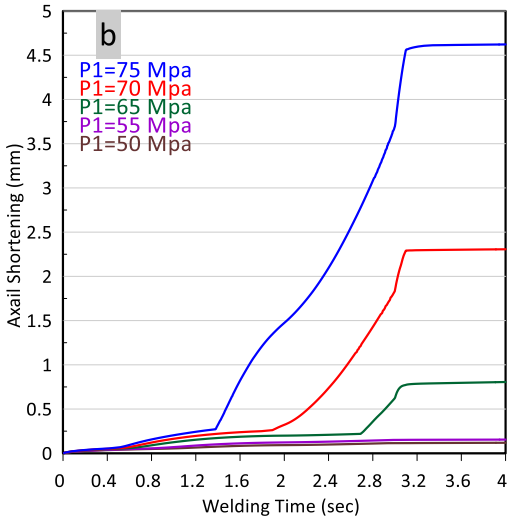

Figure 12: (a) Temperature profile variation and (b) axial shortening variation, at different frictional pressures for dissimilar joint.

6.3.2 Effect of forging pressure (P_2)

The temperature profile with time at the interface region and the variation axial shortening with time, both at different forging time are shown in Fig. 13 for similar joint and in Fig. 14 for dissimilar joint. The processing parameters for similar joint are kept constant as (P_1=30 MPa, t_1=3 sec, t_2=1 sec and N=1500 rpm) and for dissimilar joint are kept constant as (P_1=70 MPa, t1=3 sec, t2=1 sec and N=1500 rpm). It is observed that the forging pressure doesn't have any effect on the temperature profile but only on axial shortening. With increasing the forging pressure, the decreases in length will be higher. The percentage of decreasing in length is greater in a similar joint than that of a dissimilar joint, it could be because of the larger difference between frictional pressure and forging pressure for the similar joint.

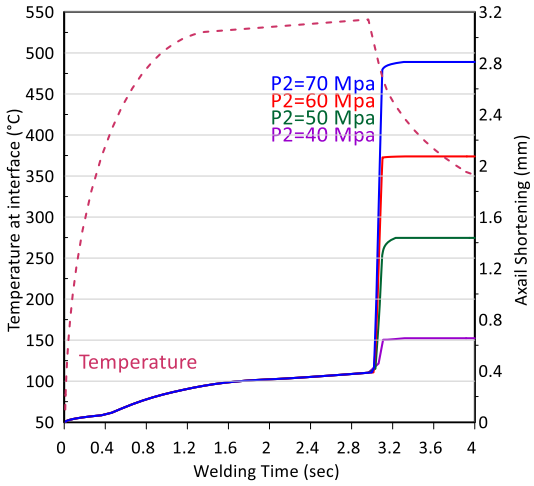

Figure 13: Temperature profile and variation of axial shortening at different forging pressures for similar Al-alloy joint.

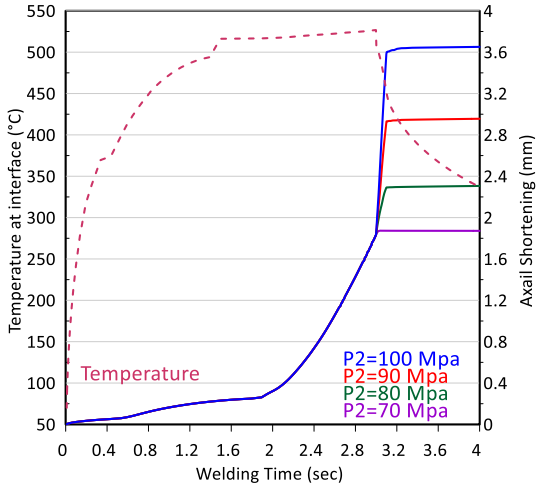

Figure 14: Temperature profile and variation of axial shortening at different forging pressures for dissimilar joint.

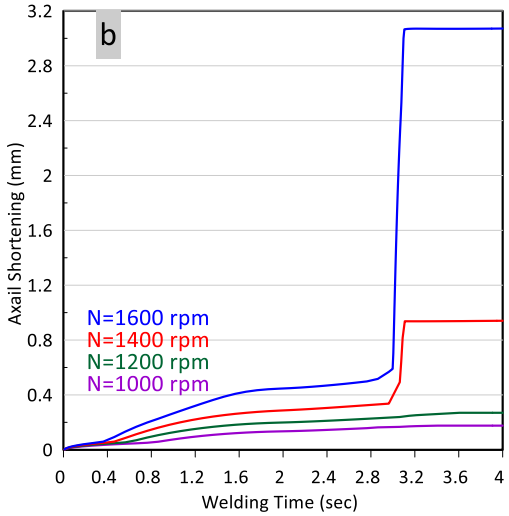

Figure 15: (a) Temperature profile variation and (b) axial shortening variation, at different rotational speeds for similar joint.

6.3.3 Effect of rotational speed (N)

The temperature profile with time at the interface region between the two rods at different rotational speed are shown in Fig. (15-a) for similar Al-alloy joint and in Fig. (16-a) for dissimilar Al-alloy/mild steel joint. The axial shortening with time for the welded rod at different frictional time are shown in Fig. (15-b) for similar joint and in Fig. (16-b) for dissimilar joint. The processing parameters for similar joint are kept constant as (P_1=30 MPa, P_2=60 MPa, t_1=3 sec and t_2=1) and for dissimilar joint are kept constant as (P_1=70 MPa, P_2=80 MPa, t_1=3 sec and t_2=1 sec). It is observed that as the rotational speed increases, the temperature at the interface will increase, and the axial shortening will also increase. The effect of rotational speed on the results for both similar and dissimilar joints is similar to that of the effect of frictional pressure.

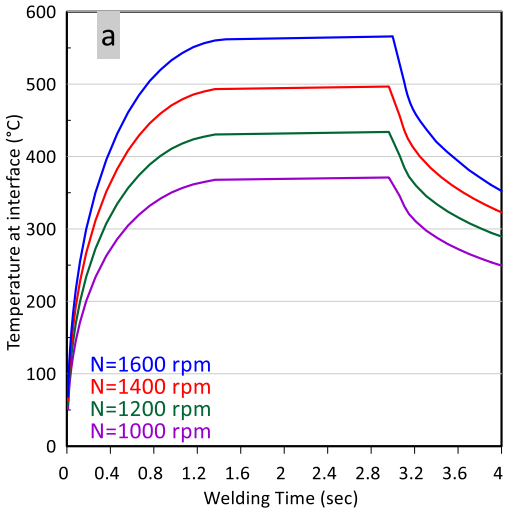

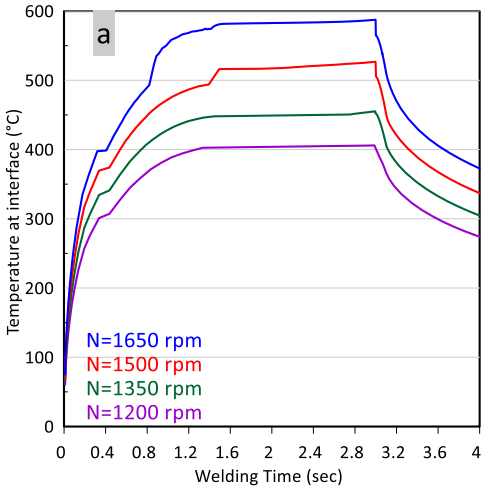

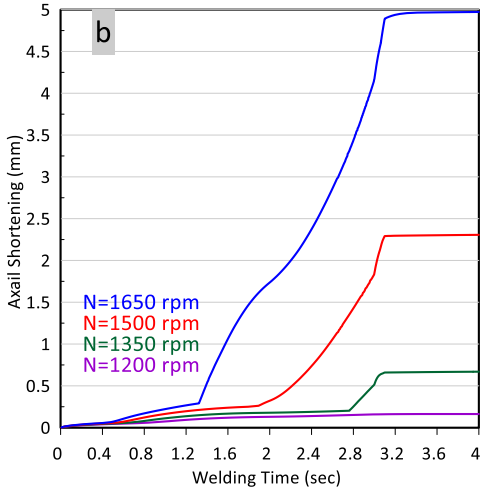

Figure 16: (a) Temperature profile variation and (b) axial shortening variation, at different rotational speeds for dissimilar joint.

6.1.4 Effect of frictional time (t_1)

The temperature profile with time at the interface region between the two rods with different frictional time are shown in Fig. (17-a) for similar Al-alloy joint and in Fig. (18-a) for dissimilar Al-alloy/mild steel joint. The variation of axial shortening with time for the welded rod at different frictional time are shown in Fig. (17-b) for similar joint and in Fig. (18-b) for dissimilar joint. The processing parameters for similar joint are kept constant as (P_1=20 MPa, P_2=40 MPa, N=1500 rpm and t_2=1) and for dissimilar joint are kept constant as (P_1=38 MPa, P_2=48 MPa, N=1500 rpm, t_2=1).It is observed that as the frictional time increases, the temperature at interface will increases too, and the axial shortening will also increases. The effect of frictional time on the results for both similar and dissimilar joint look like the effect of frictional pressure and rotational speed.

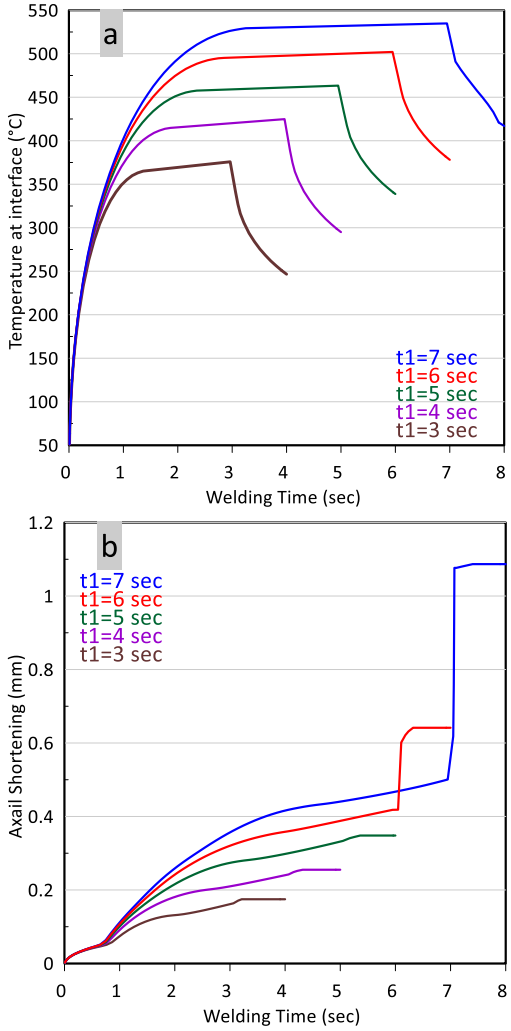

Figure 17: (a) Temperature profile variation and (b) axial shortening variation, at different frictional times for similar joint.

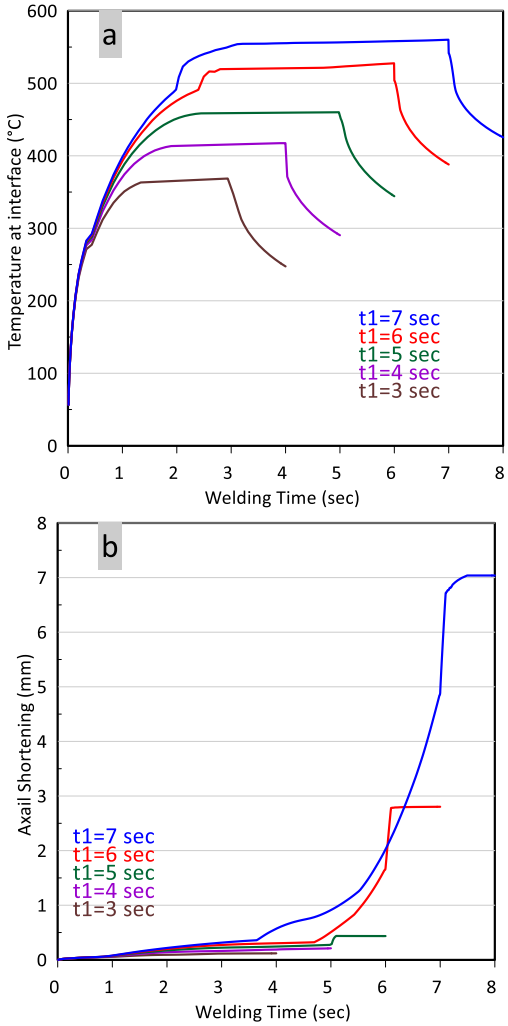

Figure 18: (a) Temperature profile variation and (b) axial shortening variation, at different frictional time's for dissimilar steel joint.

6.4 Contribution of welding parameters

Using statistic method (ANOVA-Contribution), contribution percent of processing parameters on both maximum temperature at the interface region and the axial shortening was obtained, as shown in Table (3) for similar Al-alloy joint and Table (4) for dissimilar Al-alloy/mild steel joint. For similar and dissimilar joints it is observed that the two parameters that have the most effects on the maximum temperature at the interface are frictional pressure and rotational speed, while frictional time affects less. The effect of frictional pressure is slightly more than the effect of rotational speed. Forging pressure and forging time have no effect on temperature rising at the interface probably because of the rotational stop in the third stage, so there is no heat generation. The most influential parameter on the axial shortening of the welded rod was frictional pressure, with a greater percentage for the

dissimilar joint compared with the similar joint. The forging pressure has more effect on axial shortening for similar joints compared with the dissimilar joint. The rotational speed and frictional time, have a near effect on axial shortening for both similar and dissimilar joints. Forging time has the least effect on axial shortening for both similar and dissimilar joints and it is the effect on the dissimilar joint was much lesser.

Table 3: Contribution percent of welding parameters in the similar joint.

parameters	Maximum temperature	Axial shortening
Frictional pressure	46.83%	31.38%
Rotational speed	38.32%	17.68%
Frictional time	14.85%	18.42%
Forging pressure	0%	26.2%
Forging time	0%	6.32%

Table 4: Contribution percent of parameters in the dissimilar joint.

parameters	Maximum temperature	Axial shortening
Frictional pressure	44.98%	34.34%
Rotational speed	40.99%	20.06%
Frictional time	14.03%	21.3%
Forging pressure	0%	20.36%
Forging time	0%	3.4%

7. CONCLUSION

The current research work has been studied the continuous drive rotary friction welding numerically using (ANSYS) for similar and dissimilar joints with a range of welding parameters. The most prominent results obtained were as follows:

1- In general, with increasing of welding parameters, the welding temperature at the interface region and the axial shortening of the workpiece will increases.

2- For similar and dissimilar joints, frictional pressure and rotational speed has the most effect on the welding temperature at the interface region, frictional time affects less while forging pressure and forging time has no effect on maximum temperature.

3- The most deformation happened in dissimilar welding process is for Al-alloy, because it's weaker than mild steel.

4- Contribution percent of parameters on the maximum welding temperature at the interface region were: (P_1: 46.83%), (N: 38.32%), and (t_1: 14.85%) for similar joint, and for the dissimilar joint were: (P_1: 44.98%), (N: 40.99%) and (t_1: 14.03%).

5- For similar and dissimilar joints the most influential parameter on the axial shortening was frictional pressure.

6- Contribution percent of parameters on the axial shortening were: (P_1: 31.38%), (P_2: 26.2%), (N: 17.68%), (t_1: 18.42%) and (t_2: 6.32%) for similar joint, and for the dissimilar joint were: (P_1: 34.34%), (P_2: 20.36%), (N: 20.06%), (t_1: 21.3%) and (t_2: 3.4%).

REFERENCES

[1] C. J. Brown, *An analytical model of material deformation in rotary friction welding of thin-walled tubes*. Brigham Young University, 2018.

[2] N. S. Kalsi and V. S. Sharma, "A statistical analysis of rotary friction welding of steel with varying carbon in workpieces," *Int. J. Adv. Manuf. Technol.*, vol. 57, no. 9–12, pp. 957–967, 2011.

[3] M. Maalekian, "Friction welding–critical assessment of literature," *Sci. Technol. Weld. Join.*, vol. 12, no. 8, pp. 738–759, 2007.

[4] H. Seli, A. I. M. Ismail, E. Rachman, and Z. A. Ahmad, "Mechanical evaluation and thermal modelling of friction welding of mild steel and aluminium," *J. Mater. Process. Technol.*, vol. 210, no. 9, pp. 1209–1216, 2010.

[5] M. Maalekian, E. Kozeschnik, H. P. Brantner, and H. Cerjak, "Comparative analysis of heat generation in friction welding of steel bars," *Acta Mater.*, vol. 56, no. 12, pp. 2843–2855, 2008.

[6] J. Chen and B. Young, "Stress–strain curves for stainless steel at elevated temperatures," *Eng. Struct.*, vol. 28, no. 2, pp. 229–239, 2006.

[7] Q. Li, F. Li, M. Li, L. Fu, and Q. Wan, "Finite element simulation of deformation behavior in friction welding of Al-Cu-Mg alloy," *J. Mater. Eng. Perform.*, vol. 15, no. 6, pp. 627–631, 2006.

[8] M. Murugesan and D. W. Jung, "Johnson Cook material and failure model parameters estimation of AISI-1045 medium carbon steel for metal forming applications," *Materials (Basel).*, vol. 12, no. 4, p. 609, 2019.

[9] M. A. El-Hadek, "Numerical simulation of the inertia friction welding process of dissimilar materials," *Metall. Mater. Trans. B*, vol. 45, no. 6, pp. 2346–2356, 2014.

[10] K. A. Shrikrishana and P. Sathiya, "Finite element modelling and characterization of friction welding on UNS S31803 duplex stainless steel joints,"

Eng. Sci. Technol. an Int. J., vol. 18, no. 4, pp. 704–712, 2015.
[11] P. T. Summers *et al.*, "Overview of aluminum alloy mechanical properties during and after fires, Fire Sci." Rev, 2015.
[12] P. Biswas, N. R. Mandal, O. P. Sha, and M. M. Mahapatra, "Thermo-mechanical and experimental analysis of double pass line heating," *J. Mar. Sci. Appl.*, vol. 10, no. 2, pp. 190–198, 2011.
[13] D. D. FULLER, "2d. coefficients of friction," *Am. Inst. Phys. Handb.*, vol. 1, p. 42, 1963.
[14] J. T. Xiong, J. L. Li, Y. N. Wei, F. S. Zhang, and W. D. Huang, "An analytical model of steady-state continuous drive friction welding," Acta Mater., vol. 61, no. 5, pp. 1662–1675, 2013.

تاثيرات المعاملات الاساسية للحام الاحتكاك الدوار على الخصائص الحرارية للربط المتشابه وغير المتشابه

فارس ابراهيم صالح faris.enp67@student.uomosul.edu.iq
امير سلطان داؤود asdawood54@gmail.com
عبد الحق عبد القادر حامد abdulhaqqhamid@uomosul.edu.iq

جامعة الموصل - كلية الهندسة – قسم الهندسة الميكانيكية

الملخص

في هذه البحث، تم عمل نموذج عددي لوصف تأثير معاملات (المتغيرات) الرئيسية للحام الاحتكاك الدوار على الخصائص الحرارية لكل من الربط المتشابه لسبيكة الالمنيوم (*T65*-6060) و الربط غير المتشابه سبيكة الالمنيوم (*T65*-6060) / سبيكة الصلب منخفض الكاربون من خلال برنامج (*ANSYS*). تم عمل نموذج رياضياتي يوصف الحرارة المتولدة داخل القطع نتيجة الاحتكاك والتشوه الحاصل في القطع، اثناء عملية اللحام. انتقال الحرارة خلال القطع اثناء اللحام تم توصيفها من خلال قانون فورييه للتوصيل الحراري.. المتغيرات كانت كالتالي: ضغط الاحتكاك، ضغط التشكيل، وقت الضغط، وقت التشكيل بالاضافة الى السرعة الدورانية. تم اخذ مدى مناسب للمتغيرات. نتائج التحليل العددي اظهرت انه مع زيادة قيمة المتغيرات تؤدي الى ارتفاع درجة الحرارة المتولدة بين القطعتين وكذلك تؤدي الى زيادة النقصان في طول القطع . للربط المتشابه وغير المتشابه كان لضغط الاحتكاك والسرعة الدورانية التاثير الاكبر على درجة الحرارة القصوى مع تاثير اقل لوقت الاحتكاك، اما ضغط التشكيل ووقت التشكيل فلم يكن لديهما اي تاثير على درجة الحرارة القصوى لعملية اللحام. لكل من الربط المتشابه وغير المتشابه كان ضغط الاحتكاك العامل الاكثر تاثيرا على النقصان في طول القطع، مع تاثير قليل لوقت التشكيل.

الكلمات الداله :

النمذجة العددية، لحام الاحتكاك الدوار، ملف تعريف درجة الحرارة، النقصان في الطول، معاملات اللحام.